

# A Novel On-demand Framework for Collaborative Object Detection in Sensor Networks

Guanqun Yang  
Iowa State University, Ames, IA 50011  
{gqyang}@iastate.edu

**Abstract**—In this report, we present the omitted contents in our Infocom’08 paper.

## I. PROBLEMS WITH SIMPLE COLLABORATIVE MECHANISMS FOR OBJECT DETECTION

We first investigate several simple decision fusion-based collaborative mechanisms for object detection.

### A. A Naive Collaborative Mechanism

There are two types of object detection mechanisms in sensor networks: *without collaboration* and *with collaboration* among sensors. If without collaboration, a single sentry node reports a detection to the sink when its measurement is higher than the decision threshold. We use  $T_1$  to denote the sentry node’s decision threshold where subscript ‘1’ indicates that the decision is solely based on its own measurement.

The first simple collaborative mechanism we investigate is a naive one based on [1] as follows. An object detection is reported if at least  $K$  sentry nodes sense a measurement higher than decision threshold  $T_K$ , where  $K$  is called the *collaboration degree*. Note that  $T_K < T_1$  because, in order to maintain the same false detection probability, decision threshold decreases as  $K$  increases. The false detection probability  $P_{FD}$  can be calculated by:

$$P_{FD}(K, N^a) = 1 - \sum_{m=0}^{K-1} \binom{N^a}{m} (p_{fa})^m (1 - p_{fa})^{N^a - m}, \quad (1)$$

where  $p_{fa}$  is the probability that an individual sensor raises a false alarm and equals  $(1 - F_N(T_K))$ , as shown in Fig. 1(b). Next, we calculate the expected detection probability  $E(P_D)$ ,

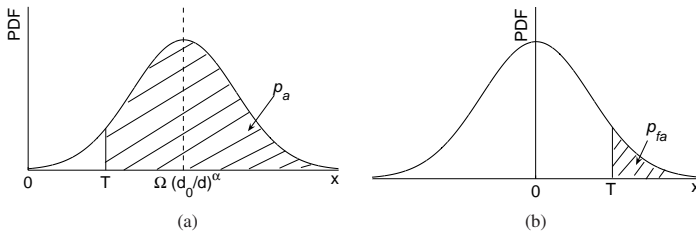


Fig. 1. (a) Probability of genuine alarm:  $p_a = P(\mathbf{x} \geq T | \mathcal{H}_1)$  and (b) probability of false alarm:  $p_{fa} = P(\mathbf{x} \geq T | \mathcal{H}_0) = 1 - F_N(T)$ , where  $\mathbf{x}$  is the sensor measurement,  $T$  is the decision threshold, and  $F_N(\cdot)$  is the cumulative distribution function of noise.

which will be denoted as  $\bar{P}_D$  in the rest of this paper. To obtain  $\bar{P}_D$ , we first need to calculate  $\bar{p}_a$ , the probability that an individual sensor senses a reading higher than  $T_K$ , given that the object is present in the region. When the size of the sensor network is sufficiently large, we can neglect the edge effect

and assume that the object is at center  $(0, 0)$  of the region  $\mathcal{R}$  without loss of generality. Thus,  $\bar{p}_a$  can be calculated by:

$$\bar{p}_a = \iint_{\mathcal{R}} \left( 1 - F_N \left( T_K - \frac{\Omega d_0^2}{x^2 + y^2} \right) \right) dx dy. \quad (2)$$

Because sensors are randomly independently distributed in the region and their readings are also independent from each other, we have

$$\bar{P}_D(K, N^a) = 1 - \sum_{m=0}^{K-1} \binom{N^a}{m} (\bar{p}_a)^m (1 - \bar{p}_a)^{N^a - m}. \quad (3)$$

Now given the target false detection probability ( $P_{FD}^*$ ), we observe through numerical studies that the expected detection probability ( $\bar{P}_D$ ) goes down as the degree of collaboration ( $K$ ) increases (as illustrated in Fig. 2). This is because, with a larger  $K$ , the increase in detection probability offered by a lower decision threshold ( $T_K$ ) is offset by the decrease in detection probability due to a larger number of sentry nodes required to raise an alarm at the same time.

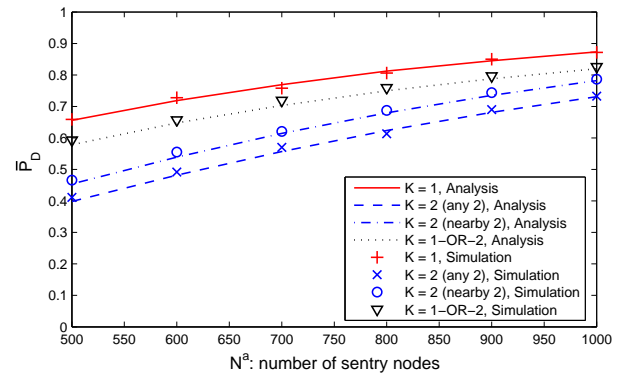


Fig. 2. Expected detection probability ( $\bar{P}_D$ ) vs. number of sentry nodes ( $N^a$ ) for various simple collaborative mechanisms. The target false detection probability is set to  $P_{FD}^* = 0.001$ . The dashed line for  $K = 2$  shows the naive scheme where any  $K$  sentry nodes can collaborate while the dash-dotted line is for the enhanced version where only nearby sentry nodes are allowed to collaborate. The dotted line shows the 1-OR-2 collaborative scheme (with an arbitrary combination of  $T_1'$  and  $T_2'$ ).

### B. An Enhancement to the Naive Collaborative Mechanism

In the above mechanism, since there is no constraint on which sentry nodes may collaborate, sentry nodes that are even far away from each other can collaborate to report a detection, thus resulting in a high  $P_{FD}$ . To improve upon this mechanism, we consider an enhancement as follows. Once a sentry node

senses a reading higher than  $T_K$ <sup>1</sup>, it queries nearby active sensors within its neighborhood called *fusion range*, which is a circle with radius of  $R_f$  centered at the sentry node. Then, a detection is reported if and only if the sentry node receives at least  $(K - 1)$  alarms from active sensors within its fusion range. Accordingly, the system's false detection probability for this scheme can be calculated by:

$$P_{FD}(K, N^a) = 1 - (1 - \mathbb{P}_{FA})^{N^a}, \quad (4)$$

where  $\mathbb{P}_{FA}$  is the probability that any sentry node reports a false detection after applying the localized decision fusion described above. Note that we treat distinct sentry nodes reporting false detections as independent events. This is reasonable because, due to the low false detection probability usually required by the system, sentry nodes that report false detection are likely far away from each other, hence their fusion ranges seldom overlap.

Next, we apply a general result from the theory of probability [2] to obtain  $\mathbb{P}_{FA}$ . According to the theory of probability, if the probability of an event  $A$  occurring in a single experiment is  $q$ , and if the number of independent experiments follows a Poisson distribution with parameter  $\lambda$ , the probability of event  $A$  occurring at least  $K$  times in the series of experiments is:

$$P = 1 - \sum_{m=0}^{K-1} \frac{e^{-q\lambda} (q\lambda)^m}{m!}. \quad (5)$$

When  $N^a$  is sufficiently large, the number of active sensors within the fusion range can be approximated by a Poisson distribution [3] with parameter  $N^a \pi R_f^2$ . Also, we know that the probability that a sensor raises a false alarm is  $p_{fa}$ . Thus, by applying the above general result from the theory of probability, we have:

$$\mathbb{P}_{FA} = p_{fa} \left( 1 - \sum_{m=0}^{K-2} \frac{e^{-p_{fa} N^a \pi R_f^2} (p_{fa} N^a \pi R_f^2)^m}{m!} \right).$$

Substituting the above result about  $\mathbb{P}_{FA}$  into (4), we complete the calculation of  $P_{FD}$ .

On the other hand, we know that, as long as there are at least  $K$  active sensors raising alarms within  $\frac{R_f}{2}$  distance to the object, a detection will always be reported according to the localized decision fusion describe above. Let  $\bar{\mathbb{P}}_A$  denote the expected probability that an active sensor, within  $\frac{R_f}{2}$  to the object, raises an alarm; we have:

$$\bar{\mathbb{P}}_A = \int_0^{\frac{R_f}{2}} \frac{1}{\pi \left(\frac{R_f}{2}\right)^2} \cdot 2\pi r \cdot \left( 1 - F_N \left( T_K - \frac{\Omega d_0^2}{r^2} \right) \right) dr. \quad (6)$$

Similarly, by applying the general result from the theory of probability, the expected detection probability  $\bar{P}_D(K, N^a)$  is then given by:

$$\bar{P}_D(K, N^a) \geq 1 - \sum_{m=0}^{K-1} \frac{e^{-\bar{\mathbb{P}}_A N^a \pi \left(\frac{R_f}{2}\right)^2} \left( \bar{\mathbb{P}}_A N^a \pi \left(\frac{R_f}{2}\right)^2 \right)^m}{m!}. \quad (7)$$

<sup>1</sup>For simplicity, we use the same notation  $T_K$  to represent the decision threshold for collaboration degree of  $K$  when we describe different collaborative mechanisms in Sections I-A and I-B, though the actual value of  $T_K$  varies with the mechanism. This is because the group of  $K$  sensors participating in collaboration is different in different schemes. Similarly, we reuse the notations  $p_a$ ,  $p_{fa}$ ,  $\mathbb{P}_{FA}$ ,  $\bar{\mathbb{P}}_A$ ,  $P_{FD}$ ,  $\bar{P}_D$ , and  $R_f$ .

Though this enhancement improves upon the naive one still it gives inferior performance to the simple mechanism without collaboration (as shown in Fig. 2), regardless of the size of the fusion range ( $R_f$ ). Fig. 2 plots the analytical and simulation results with  $R_f$  set to 0.1 units. To better understand the rationale, Fig. 3 shows the coverage region (according to our definition of point information coverage) of two neighboring active sensors in different scenarios. Comparing Fig. 3(a) with Figs. 3(b) and 3(c), we can see that the coverage region shrinks when two sensors collaborate with each other. In addition, we find that collaboration is beneficial only when two sensors are very close to each other.

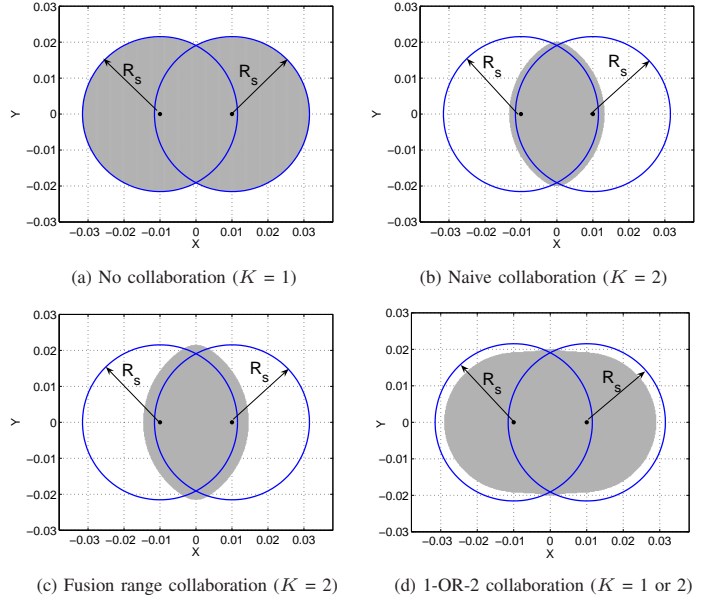


Fig. 3. Coverage region (shown as shaded area) of two neighboring active sensors (apart by 0.02 units) in different scenarios. When  $K$  equals 1, a single sensor's coverage region is a disk with radius  $R_s$  centered at itself. The detection thresholds used in these four scenarios result in the same false detection probability. Notice that the coverage regions in (b), (c) and (d) are all smaller than that in (a).

At last, we study a 1-OR-2 collaborative scheme ( $K = 1$  or 2) where an object detection is reported if at least one sentry node has sensed a reading higher than  $T'_1$  or at least two sentry nodes have measurements larger than  $T'_2$  ( $T'_2 < T'_1$ ). The calculations of  $P_{FD}$  and  $\bar{P}_D$  are similar to the analysis above, and the calculation details are omitted due to space limitation. Note that, due to the 'OR' operation,  $T'_1$  and  $T'_2$  are different from  $T_1$  and  $T_2$ . Moreover, there is a fixed relation between  $T'_1$  and  $T'_2$  in order to achieve the target false detection probability. We exploit different combinations of  $T'_1$  and  $T'_2$  and through numerical studies, we observe that this scheme also yields worse performance than the simple scheme without collaboration (i.e.,  $K = 1$ ) regardless of the choices for  $T'_1$  and  $T'_2$ . This is because, the increase in detection probability by introducing collaboration is offset by the decrease in detection probability due to use of higher  $T'_1$  and  $T'_2$  to maintain the same target false detection probability. Fig. 2 plots the results with an arbitrary combination of  $T'_1$  and  $T'_2$  and Fig. 3(d) shows the coverage region of two neighboring sensors with the 1-OR-2 collaborative scheme. Similarly, performances of other com-

bination schemes (e.g., 2-OR-3, 1-OR-2-OR-3, etc) are also worse than that of the simple scheme without collaboration.

### C. Simulation-based Validation

The analytical studies in Sections I-A and I-B are validated by simulation results shown in Fig. 2. In the simulation, the object's source model is characterized by  $\Omega = 2100$  mW and  $d_0 = 0.001$  units, and the background noise follows a normal distribution  $\mathcal{N}(0, \sigma^2)$  with  $\sigma = \sqrt{2}$  mW. The target  $P_{FD}^*$  is 0.001. We test 100 different deployments. In each deployment, sensors are randomly deployed in a  $1 \times 1$  unit area; we randomly select 100 locations for the object, and simulation is repeated 1000 times for each location. All simulation results match the analytical results very well.

Through above analytical and simulation studies, we note that the naive collaboration mechanism and its enhancements do not help improve the object detection performance. On the other hand, we suspect that better detection performance may be achieved if the collaboration among sensors is planned carefully. This motivates us to develop an on-demand framework for decision fusion-based collaborative object detection.

## II. ENERGY EFFICIENCY STUDY OF THE PROPOSED ON-DEMAND COLLABORATIVE FRAMEWORK

In this section we investigate the network energy efficiency performance when the proposed framework is adopted.

### A. Design Objective

Let  $\mathcal{P}(K, N_K^a, N_K^i)$  denote the power consumption for a wireless sensor network operating with our proposed framework, where  $K$  is the collaboration degree,  $N_K^a$  is the number of sentry nodes and  $N_K^i$  is the number of inert nodes. The objective is to find the optimal pair  $(\hat{N}_K^a, \hat{N}_K^i)$  for a given  $K$ , which minimizes the network power consumption while guaranteeing a target  $\rho^*$ -coverage of the region. Here, we treat  $K$  as a design preference for specific applications; for example, when locating or tracking objects, a large  $K$  may be preferred for accurate results. The requirement of  $\rho^*$ -coverage [4] can be translated into the requirements of  $P_{FD}$  and  $\bar{P}_D$ :

$$P_{FD}(K, N_K^a, N_K^i) \leq P_{FD}^* \text{ and } \bar{P}_D(K, N_K^a, N_K^i) \geq P_D^*, \quad (8)$$

where  $P_{FD}^* = P_{FD}^{\max}$  and  $P_D^* = (\rho^* + (1 - \rho^*)P_D^{\min})$ . Recall that  $P_{FD}^{\max}$  and  $P_D^{\min}$  are the maximum false detection probability and the minimum detection probability which are used to define point information coverage and  $\rho$ -coverage. Formally, this design problem is stated as follows.

**Given  $K, P_{FD}^*$ , and  $P_D^*$ , determine:**

$$(\hat{N}_K^a, \hat{N}_K^i) = \arg \min_{\substack{P_{FD}(K, N_K^a, N_K^i) \leq P_{FD}^* \\ \bar{P}_D(K, N_K^a, N_K^i) \geq P_D^*}} \mathcal{P}(K, N_K^a, N_K^i). \quad (9)$$

**Hence,**  $\mathcal{P}^*(K) = \mathcal{P}(K, \hat{N}_K^a, \hat{N}_K^i).$  (10)

The calculation of  $\mathcal{P}(K, N_K^a, N_K^i)$  will be discussed in Section II-C. In this paper, we only consider the power consumption for sensing, collaborative decision making and sensor's regular operation e.g. CPU and radio. The power consumed for a sentry node to report its detection to the sink is not considered as it varies with the routing and aggregation methods used. Once the methods are known, they can be incorporated into our power consumption analysis without much difficulty.

### B. Observations and Simplification

The problem stated above is very complex and here we present some interesting observations that help simplify the problem.

- For a given collaboration degree  $K$ , there exists a minimum number of sentry nodes ( $\hat{N}_K^a$ ) required to meet the system probability constraints:

$$\hat{N}_K^a = \arg \min_{\substack{P_{FD}(K, N_K^a, N_K^i) \leq P_{FD}^* \\ \bar{P}_D(K, N_K^a, N_K^i) \geq P_D^*}} N_K^a, \quad \forall K \geq 1. \quad (11)$$

- For a given collaboration degree  $K$  and number of sentry nodes  $N_K^a \geq \hat{N}_K^a$ , there exists a minimum number of inert nodes ( $\hat{N}_K^i$ ) required to meet the system probability constraints:

$$\begin{aligned} \hat{N}_K^i(N_K^a) &= \arg \min_{\substack{P_{FD}(K, N_K^a, N_K^i) \leq P_{FD}^* \\ \bar{P}_D(K, N_K^a, N_K^i) \geq P_D^*}} N_K^i \\ &= \arg \min_{\substack{P_{FD}(K, N_K^a, N_K^i) \leq P_{FD}^* \\ \bar{P}_D(K, N_K^a, N_K^i) \geq P_D^*}} \mathcal{P}(K, N_K^a, N_K^i). \end{aligned} \quad (12)$$

The second equality in (12) is based on the fact that given the number of sentry nodes and collaboration degree, less inert nodes result in lower network power consumption.

Further, when  $N_K^a = \hat{N}_K^a$ ,  $\hat{N}_K^i(\hat{N}_K^a) = \hat{N}_K^i$ .

With the help of above observations we are able to simplify our design problem and make the search space for optimal  $(\hat{N}_K^a, \hat{N}_K^i)$  significantly smaller. The original problem given by (9) can now be restated as:

$$(\hat{N}_K^a, \hat{N}_K^i) = \arg \min_{\substack{N_K^a \geq \hat{N}_K^a \\ N_K^i = \hat{N}_K^i(N_K^a)}} \mathcal{P}(K, N_K^a, N_K^i). \quad (13)$$

### C. Calculation of $\mathcal{P}(K, N_K^a, N_K^i)$

In Table I, we summarize the notations to be used in Sections II-C and II-D. Please note that  $\mathcal{P}_{sentry}$  is equal to  $(\mathcal{P}_{sense} + \mathcal{P}_{active})$ , while  $P_{inert} = \mathcal{P}_{active}$  for message-based inert node model and  $P_{inert} = \mathcal{P}_{sleep}$  for circuit-based inert node model. For the message-based inert node model, the power consumption for the network can be easily derived as:

$$\mathcal{P}(K, N_K^a, N_K^i) = \begin{cases} \mathcal{P}_{sentry} N_1^a, & K = 1, \\ \mathcal{P}_{sentry} N_K^a + \mathcal{P}_{inert} N_K^i + \\ ((1 - P(\mathcal{H}_1))(1 - E_N(T_K)) + \\ P(\mathcal{H}_1)P_n\bar{P}_A + \\ P(\mathcal{H}_1)(1 - P_n)(1 - E_N(T_K))) \times \\ N_K^a (E_f(K) + N_K^i R_f^2 \pi \mathcal{P}_{sense} \tau) f_s, & K > 1. \end{cases} \quad (14)$$

TABLE I  
NOTATIONS FOR CALCULATING NETWORK POWER CONSUMPTION

Notation	Remarks
$\mathcal{P}_{sense}$	Power consumption for sensing task by each sensor.
$\mathcal{P}_{active}$	Power consumption, except sensing, for each active sensor.
$\mathcal{P}_{sleep}$	Power consumption for a sensor in sleeping state.
$f_s$	Sensing frequency for sentry node.
$E_f(K)$	Average energy consumption for executing one triggering process.
$E_{msg}$	Energy consumption for transmitting one message.
$P(\mathcal{H}_1)$	Probability that object is present in the network.
$P_n$	Probability that a sentry node is in D.Z. $P_n = (R_f/2)^2 \pi$ .
$\bar{P}_A$	Prob. that a sensor in D.Z. has measurement $> T_K$ .
$\tau$	Time required to acquire a single sensor reading.

For the circuit-based inert node model, the power consumption can be calculated by (14) after the calculation of  $E_f(K)$  is properly adjusted. Since the inert nodes are already awake in the message-based model, no energy is required to wake them up and  $E_f(K)$  is simply the energy required for decision fusions. However, in the circuit-based model, in addition to the energy consumed for decision fusions, the sentry nodes consume extra energy for triggering the inert nodes within its fusion range [5].

#### D. Numerical Study and Simulation-based Validation

First, through numerical studies we offer some interesting insights on how the network energy efficiency performance varies with the inert node model, the collaboration degree and various parameters discussed in previous sections. Table II lists the system parameters used for this study. Using these

TABLE II  
SYSTEM PARAMETERS USED IN NUMERICAL AND SIMULATION STUDIES

Parameter	Value	Remarks
$\Omega$	2100 mW	Signal amplitude of the object.
$d_0$	0.001 unit	A constant.
Noise	-	$\mathcal{N}(0, \sigma^2)$ where $\sigma = \sqrt{2}$ mW.
$f_s$	1 Hz	Sensing frequency for sentry node.
$E_{msg}$	2.23 mJ	Energy consumed to transmit one message.
$P(\mathcal{H}_1)$	0.9	Probability that object is present.
$\tau$	30 ms	Time required to acquire a single sensor reading.

parameters, for  $K = 1$  we obtain  $\hat{N}_1^a = 1114$  and the corresponding power consumption  $\mathcal{P}^*(1)$  is  $3.453 \times 10^5$  mW. In the remaining of this section, all power consumptions are normalized over  $\mathcal{P}^*(1)$ . The solution to the optimization problem defined in Eq. (13) determines the optimal pair  $(\hat{N}_K^a, \hat{N}_K^i)$  for a given  $K$ . Particularly, Fig. 4(a) shows the variation of network power consumption, when  $K$  is 5, with the number of sentry nodes varying from  $\hat{N}_5^a$  to  $\hat{N}_1^a$ . The results are shown for a fixed ratio of  $\mathcal{P}_{sense}/\mathcal{P}_{active} = 4$  ( $\mathcal{P}_{sense} = 248$  mW,  $\mathcal{P}_{active} = 62$  mW). We see that, for the message-based inert node model,  $\hat{N}_5^a = 655$  yields the lowest network power consumption of  $\mathcal{P}^*(5) = 0.936$ , and the corresponding  $\hat{N}_5^i$  is 1800. Further, we see that  $\hat{N}_5^a = 620 < 655 = \hat{N}_5^a$ . This is because when  $N_K^a$  decreases,  $N_K^i$  increases to satisfy the system probability constraints; since inert nodes consume a considerable amount of power in the message-based inert node model, a smaller  $N_K^a$  may not necessarily result in lower network power consumption.

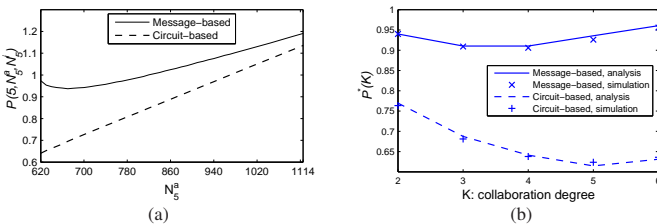


Fig. 4. (a) Given  $K = 5$ , normalized network power consumption ( $\mathcal{P}(5, N_5^a, N_5^i)$ ) vs. number of sentry nodes ( $N_5^a$ ), with  $N_5^a$  varying from 620 ( $\hat{N}_5^a$ ) to 1114 ( $\hat{N}_1^a$ ) and the corresponding  $N_5^i$  is equal to  $\hat{N}_5^i(N_5^a)$ . (b) Normalized optimal network power consumption  $\mathcal{P}^*(K)$  for different  $K$  and inert node models.

However, for the circuit-based inert node model, we find the lowest power consumption is achieved when  $\hat{N}_5^a = \hat{N}_5^a$  and, interestingly, the power consumption increases almost linearly with  $N_5^a$ , which is totally different from that for the message-based model. This is because, although a lower  $N_5^a$  requires a larger  $N_5^i$ , sleeping inert nodes consume much less power than sentry nodes. So, using the smallest number of sentry nodes always yields the lowest network power consumption. The results for other collaboration degrees are similar with the above case.

We further simulate the optimal power consumption under various collaboration degrees for validation purpose. We simulate 10 different deployments, where  $N_K^a = \hat{N}_K^a$  and  $N_K^i = \hat{N}_K^i$  for each  $K$ . We simulate the message-based and circuit-based models for 1000 sensing cycles each with  $P(\mathcal{H}_1) = 0.9$ . Simulation results are normalized and plotted in Fig. 4(b), which are very close to the analytical results.

Although we leave the decision of choosing a proper  $K$  to the system designer, to give an insight on how  $K$  affects the optimal power consumption in our proposed framework, we conduct a numerical study of network power consumption with variation in the ratio  $\mathcal{P}_{sense}/\mathcal{P}_{active}$  for various  $K$ . Figs. 5 (a) and (b) show the trends for message-based and circuit-based inert node models respectively. Suppose the collaboration degree yielding the lowest power consumption is  $K^*$ . It is observed that  $K^*$  varies with the ratio  $\mathcal{P}_{sense}/\mathcal{P}_{active}$ . For the message-based model, if the ratio is below 1, we find that  $K^*$  is always 1 because inert nodes consume a considerable amount of energy for regular operation. However, when the ratio goes beyond 2, schemes with higher degree of collaboration start performing comparably to or even better than the non-collaboration scheme. This happens because the power consumption for regular sensing becomes dominant and schemes with higher degree of collaboration are able to work with a smaller number of sentry nodes compared to the non-collaboration scheme. This also explains why when the ratio is large enough, optimal network power consumption for different  $K$  is almost proportional to  $\hat{N}_K^a$  (see Table III).

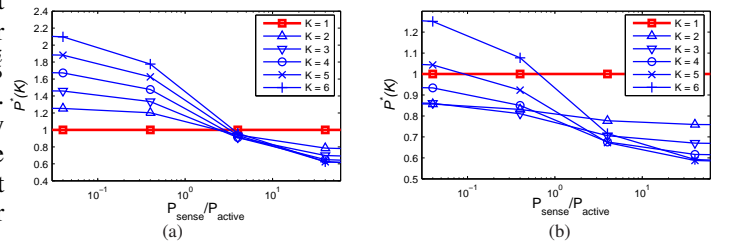


Fig. 5. Normalized optimal network power consumption  $\mathcal{P}^*(K)$  vs.  $\mathcal{P}_{sense}/\mathcal{P}_{active}$  for (a) message-based and (b) circuit-based inert node model.

TABLE III  
 $\mathcal{P}^*(K)$  AND  $\hat{N}_K^a$  FOR VARIOUS  $K$  WHEN  $\frac{\mathcal{P}_{sense}}{\mathcal{P}_{active}} = 40$

$K$	1	2	3	4	5	6
$\hat{N}_K^a$	1114	840	735	665	620	610
$\mathcal{P}^*(K)$	1	0.7594	0.6684	0.6125	0.5806	0.5803

For the circuit-based model, we also find that, in general, the network power consumption for collaborative schemes ( $K > 1$ ) decreases with the ratio  $\mathcal{P}_{sense}/\mathcal{P}_{active}$ . However, since the

time required to trigger an inert node with respect to distance increases according to power law, sentry nodes consume much more energy for triggering the inert nodes than that for sensing and operation when the fusion range is large. As higher degree of collaboration usually results in a larger fusion range, this makes the overall network power consumption very large. In Fig. 5(b), we can see that for our setup, when the ratio  $\mathcal{P}_{sense}/\mathcal{P}_{active}$  is low, power consumption for high-degree collaborations  $K = 4, 5, 6$  is even higher than that for  $K = 3$ . However, when the ratio is large enough, the sensing power becomes the dominant factor and the curves follow the same trend as for the message-based model.

We also conduct numerical and simulation studies for different  $P(\mathcal{H}_1)$  but the results do not vary much. This seems counterintuitive at the first sight but can be explained as follows. Since we consider the presence of only one object in the network and due to the low  $P_{FD}^{max}$  in our setup, D.Z. of an object is very small compared to the network size. So the portion of sensors affected by presence of an object is only a very small fraction and hence, the contribution of  $P(\mathcal{H}_1)$  to the network power consumption is small. Please note that this observation does not always hold; e.g., when the network size is small, the impact of  $P(\mathcal{H}_1)$  may be more significant.

#### E. Summary

We summarize the key observations for the proposed on-demand collaborative framework as follows.

- The circuit-based inert node model usually renders better network energy efficiency than the message-based model.
- For a given  $K$ , the smallest number of sentry nodes and inert nodes required to guarantee  $\rho^*$ -coverage may not result in the lowest network power consumption.
- With both inert node models, higher  $K$  does not always yield lower network power consumption.
- Collaboration among sensors is preferred when  $\mathcal{P}_{sense}$  is high compared to  $\mathcal{P}_{active}$ .

#### REFERENCES

- [1] T. Clouqueur, K. K. Saluja, and P. Ramanathan, "Fault Tolerance in Collaborative Sensor Networks for Target Detection," *IEEE Transactions on Computers*, vol. 53, no. 3, pp. 320–333, 2004.
- [2] S. C. Port, *Theoretical Probability for Applications*. John Wiley & Sons, 1994.
- [3] P. Hall, *Introduction to the Theory of Coverage Process*. John Wiley & Sons, 1988.
- [4] G. Yang, V. Shukla, and D. Qiao, "Analytical Study of Collaborative Information Coverage for Object in Sensor Networks," in *IEEE SECON*, 2008.
- [5] L. Gu and J. Stankovic, "Radio-Triggered Wake-Up Capability for Sensor Networks," in *Proc. IEEE RTAS*, Apr. 2004.